Structural evaluation of radially expandable cardiovascular stents encased in a polyurethane film

Steve Trigwell,[1*] Samiran De,[2] Rajesh Sharma,[2] Malay K. Mazumder,[2]

Jawahar L. Mehta[3]

[1] Electrostatics and Surface Physics Laboratory, YA-C2-T,

Kennedy Space Center, Florida, 32899

* Phone: 321-867-1222, Fax: 321-867-4489. E-mail: trigws@kscems.ksc.nasa.gov

[2] Department of Applied Science, University of Arkansas at Little Rock,

2801 S. University Avenue, Little Rock, Arkansas 72204

[3] Division of Cardiovascular Medicine, University of Arkansas for Medical Sciences,

4301 West Markham Street, Little Rock, Arkansas 72205

Abstract: A method of encasing cardiovascular stents with an expandable polyurethane coating has been developed to provide a smooth homogeneous inner wall allowing for a confluent growth of endothelial cells. In this design, the metal wire stent structure is completely covered by the polyurethane film minimizing biocorrosion of the metal (stainless steel or nitinol), and providing a homogeneous surface for surface treatment and incorporation of various eluting drugs to prevent platelet aggregation while supporting endothelialization. The polyurethane surface was treated with a helium plasma for sterilization and promotes growth of cells. The paper details the performance of the coated film to expand with the metal stent up to 225 % during deployment. We present stress/strain behavior of polyurethane films, and subsequent plasma treatment of the surface and the adhesion of the coating to the stent structure upon expansion. A film of less than 25 μm was found to be sufficient for corrosion resistance and flexibility without producing any excess stress on the stent structure. Straining the film to 225 % and plasma modification did not affect the mechanical and surface properties while allowing for improved biocompatibility as determined by the critical surface tension, surface chemistry, and roughness.

Keywords: Cardiovascular stent, restenosis, polyurethane, endothelial cells, stress/strain

INTRODUCTION

Regrowth of the atherosclerotic plaque and reblocking (reclusion or restenosis) of the artery after percutaneous transluminal coronary angioplasty (PCTA) can occur soon after the procedure, occurring in about 15 - 30 % of patients receiving cardiovascular stents.[1] Restenosis is due primarily to neointimal hyperplasia.[2] The stent also causes injury to the endothelium which can cause inflammation and consequent smooth muscle cell growth.[3] To prevent restenosis, various techniques involving coating stents with anti-thrombotic drugs have been deployed.[1, 4-6] There are two main types of stents that are in use today; balloon-expanding and self-expanding. Balloon-expanding stents are commonly manufactured from 316L stainless steel, and the self-expanding ones from an equi-atomic nickel-titanium (NiTi) alloy also known as nitinol. The material of choice at present is 316L stainless steel, but there is a recent trend towards nitinol stents.[7] Numerous studies have been performed on the biocompatibility of both 316L stainless steel and NiTi.[8-10] 316L stainless steel (Ni ~ 14 wt. %) is generally accepted as an implant material, but due to the high nickel content of NiTi alloy (Ni ~ 45 wt. %), concern exists regarding the release of Ni^{2+} ions into the body that can cause severe cellular inflammation and become a possible carcinogen over long term exposure.[11] However, finishing surface treatments such as electropolishing and passivation, and heat treatment have been shown to provide an acceptable biocompatible surface finish for NiTi.[12-13]

The present strategy has been to use various polymers, and then incorporate the drugs into the polymer matrix to prevent growth of underlying smooth muscle cells. Unfortunately, most polymers are not blood compatible and can cause an intense inflammatory response in

the artery.[14] Polyurethanes have been extensively used in biomedical research[15] and offer excellent mechanical properties and biocompatibility. Biologically active endothelial cells have the inherent property of inhibiting platelet aggregation, inflammation and inhibiting smooth muscle cell growth.

In order to provide a homogeneous endothelial cell lining on the inner wall of the encased stent, it will be necessary to provide a blood-compatible surface for growth of a bioactive endothelial cell lining to provide such antithrombegenic properties such as release of prostacyclin and NO emission and thrombomodulin. All stents in current use are based on an open-cell mesh structure that is expandable, but this open cell structure does not allow for a continuous and smooth endothelial cell lining. In order to have a homogeneous endothelial cell lining, a continuous film rather than a mesh may be preferred. A thin polymer coating that encases the metallic stent for rapid endothelialization has been developed by our group (Figure 1).[16] ChronFlex AR®, a medical grade polyurethane from Cardiotech International, Woburn, MA, was chosen for use. This polyurethane exhibits superior corrosion resistance and stress-cracking under harsh environments (the human body). It has an elongation of 500 % and tensile strength of 57 MPa and is considered ideal in applications requiring exceptional flexure endurance.[17] Previous work by Mazumder *et al.*[18] showed that a 30 μm thick coating of this polyurethane significantly reduced the corrosion susceptibility of NiTi in Ringer's solution. The most important requirement of the choice of the film encasing the stent is to support a bioactive confluent endothelial cell growth and the adhesion of the cell lining with the film surface under the physiological flow conditions. In a parallel study, the endothelial cell growth properties were investigated for this encased stent design and was

reported by De *at el.*[19] The study also showed that modification of the polyurethane film surface by helium plasma treatment enhanced the endothelial cell growth compared to untreated film.

A polymer film encasing a stent has to be a radially and uniformally expandable during angioplasty, and it must retain its integrity once expanded within the artery for its lifetime. The radial expansion and physiological performance of the polymer coating depends upon both the stent material and the film used.

A stent, encased or open cell-structured, may be considered a tube that is expanded by pressure. Pressures applied to any cylindrical structure result in hoop stress, or circumferential-loading of the tube. Both the applied pressure and the resulting hoop stress have the same units but differ in direction, as shown in Figure 2.

The hoop stress (σ) is given by:[20]

$$\sigma = P\phi/2t \qquad (1)$$

where ϕ is the tube diameter and t the coating wall thickness. The hoop force in the coating wall is given by:[21]

$$F_\theta = \sigma t L \qquad (2)$$

Where L is the length of the tube. The hoop force per unit length of the tube is:

$$f_\theta = F_\theta/L = \sigma t = P\phi/2 \qquad (3)$$

In the case of encased stents, the hoop force is of interest as it relates to the strength or maximum hoop load that can be carried by the film without failure. Failure would occur when the hoop stress exceeds the ultimate tensile strength (UTS) of the polymer coating.

The stiffness of the stent is an important quantity as it describes the effectiveness of the stent in resisting diameter loss once expanded, the balloon is removed and the stent is subjected to the blood vessel recoil. The stiffness is defined as the hoop force per unit length required to elastically change its diameter, given by;

$$K_\theta = f_\theta / d\phi \qquad (4)$$

Where $d\phi$ is the differential increment of the diameter ϕ.

Self-expanding stents are typically manufactured at the vessel diameter or slightly greater, and then crimped until used. Upon delivery to the vessel, the constraint is removed. A balloon is still deployed, but the self-expansion of the SMA assists the balloon expansion, compared to that of a stainless steel balloon-expandable stent that resists the balloon's expansion

The detailed behavior of the interaction of the balloon and self-expanding stents with the arterial wall during deployment has been investigated by Duerig *et al.*[21,22] In both cases, once the balloon is deflated, the vessel and stent recoil to establish a final stress equilibrium which depends upon the stent's stiffness, otherwise, further recoil would occur. In the examples given, for a 4 mm balloon-expandable stent expanding to 9 mm in a 7 mm vessel, and for a 10.5 mm long self-expanding stent that was crimped and expanded in a 7 mm vessel, the hoop force at the final equilibrium point is approximately 0.11 N/mm.[22] Dynamic effects after deployment due to the diastolic and systolic pressures cause variations of the equilibrium force up to +/- 0.06 N/mm.[21] A cross-section of an expanding stent is shown in Figure 3. Here the coating and stent struts are expanded by the balloon from diameter **a** to **b**. Upon deflation of the balloon, the hoop stress and the arterial wall stress compress the stent

and coating back to diameter **c**. With the balloon now not supporting the coating film, it will be likely to minimize strain by flattening out as shown with residual stresses acting in tension upon the stent framework.

Using the examples above, an encased stent with a diameter of 4 mm, and expanded to 9 mm, the polymer film would, therefore, undergo an expansion of 225 % with a residual strain of ~ 206 % after recoil. It is, therefore, of great importance that the polymer coating is able to withstand that strain and retain its integrity once expanded without causing acute recoil of the stent. Similarly, the film will have to retain its bond to the stent metal structure under strain for its lifetime. The bond strength or film adhesion, therefore, plays an important role. In addition, the final surface structure of the inner wall of the encasing film needs to be suitable for the adhesion of the endothelial cell lining. The surface roughness and wettability of the film after expansion and recoil needs to be addressed. Also, any effect of the surface modification such as plasma treatment, necessary for endothelial cell linings, on the surface chemistry and topography needs to be investigated.

Experimental studies were performed to characterize the polyurethane for use as an encased stent coating. Experimental data are presented on: The stress/strain behavior of the polyurethane coating strained to 225 % elongation, 2) the adhesion of the coating to a stent wire upon expansion, 3) the surface structural changes caused by the expansion, and, 4) The effect of surface chemistry and surface structure and wettability of the polyurethane film after surface plasma modification and expansion.

EXPERIMENTAL METHODS

Stress/strain behavior of polyurethane films

Thin films of ChronoFlex® AR polyurethane were prepared on polytetrafluoroethylene (PTFE) flat sheets by dip coating and leaving the films hanging to dry at 60 - 80 °C for 24 hours. By this method, films as thin as 30 μm can be prepared. Repeated dip coatings prepared films of various thicknesses. When cured, the films were then easily peeled off the PTFE. Strips of film 50 mm in length and 6 mm in width were cut out. The thickness of each strip was measured at ten points using a Fischer Instruments Permascope eddy current probe and the mean value taken. Tensile (stress/strain) tests were performed (ASTM D-412 standard) in an Instron 5500R equipped with an environmental chamber. The films were tested at 37°C to simulate body temperature at a strain rate of 5 mm/min. The films were strained to 225 % as measured by a video extensometer set up outside the environmental chamber. At 225 % strain, the film was unloaded at -5 mm/min until the applied load reached zero.

Effect of strain on the surface chemistry of the polyurethane coating,

Helium plasma surface modification

Plasma treatment was carried out on polyurethane films prepared as above in an atmospheric plasma generator consisting of a 90 cm long cylindrical Pyrex tube with an inner diameter of 3 cm, with copper electrodes (7.5 cm x 3 cm) placed on either side of the cylinder. The inlet to the cylinder was connected to a gas flow regulator, and the outlet to a vacuum (~10^{-2} torr). The thin polyurethane films of approximately 70 mm in length and 10 mm in width were placed onto PTFE sheets inside the cylinder within the electrode region, as shown in Figure

1. The electrodes were capacitively coupled to a power source of 12 kVrms at a frequency of 700 Hz. Helium was introduced into the tube until a characteristic glow was observed. The films were exposed for 4 and 6 minutes.

XPS analysis

Two sets of thin polyurethane films were prepared on 22 mm square glass slides that were a suitable size for submission into the ESCA spectrometer. One set was helium plasma treated for 4 and 6 minutes. The XPS data were obtained on a Kratos Axis ESCA Spectrometer using a Mg Kα ($h\nu$ = 1253.6 eV) x-ray source. The x-ray beam used was 100W, 100 mm in diameter. The collected data were referenced to Au at 84.0 +/- 0.05 eV and the C1s peak to 284.6 eV. The high-resolution scans of the C1s peaks were acquired at a pass energy of 40 eV, in 0.2 eV steps with a 3000 ms dwell time. The relative atomic concentrations of the detected elements were calculated and normalized to 100% using sensitivity factors supplied by the instrument manufacturer from known certified standards. Detection limits for XPS are approximately 0.05 to 1.0 atomic % depending upon the sensitivity of the elements. The individual element spectra were converted to ASCII format and imported to a computer where the peak curve fitting was performed using Thermo VG Scientific Eclipse V3.0 XPS data reducing software.

Surface wettability measurements

In general, there are three macroscopic properties of a surface of a solid containing more than one chemical element: the surface tension, the surface stress, and the specific surface free energy.[23] The surface tension γ is defined as the reversible work done in creating a unit area of new surface at constant temperature, volume and total number of molecules. For a solid

undergoing an isotropic strain, it will not deform isotropically as some directions on the surface will deform more easily than others; therefore, the surface tension will vary with the strain. The surface roughness will also change under strain due to the flattening out of the peaks and valleys, and it is well known that surface roughness is also a factor on the surface tension[24] The critical surface tension (γ_{crit}), as defined by Zisman,[25] is that in which the liquid has a surface tension equal to, or less than, the value required to completely wet and spread spontaneously on the surface. Baier[26] established a correlation between the critical surface tension and thrombogenicity in which there is a region of minimum γ_{crit} where biological interaction between the body and the biomaterial is at a minimum

A small platform was designed in which a length of polyurethane film can be strained to different amounts and clamped, as shown in Figure 5. A VCA-optima Surface Analysis System was used for contact angle measurements. Contact angle measurements of a homologous series of organic liquids were used to estimate the critical surface tension of an untreated polyurethane surface.[27,28] The critical surface tension was obtained by carrying out contact angle (θ) measurements for different liquids and extrapolating the data to $\cos\theta = 1$. Calibration of the VCA Optima instrument was conducted using a PTFE substrate and de-ionized water under ambient conditions (50 % RH, 20-25° C). The PTFE surface was cleaned sequentially with acetone, methanol, and distilled water. The cleaned PTFE was preserved in a hot air oven. De-ionized water droplets were generated on the PTFE surface using a Hamilton-make syringe. The droplet volume varied from 4 to 5 micro-liters. Images of droplets were acquired immediately on contact of the droplet with the PTFE surface. Each time five markers were placed around the droplet image and both right and left angle images

were calculated using the software. This process was repeated until the difference between the right and left angles was found to be minimum (< 1^0). The series of homologous organic liquids with their respective surface tensions[27,29] used for generating the Zisman plots were; de-ionized water (72.8 dynes/cm), glycerol (64.0 dynes/cm), ethylene glycol (47.7 dynes/cm), formamide (58.2 dynes/cm), and benzene (28.88 dynes/cm). The contact angle experiments on plasma-treated polyurethane were carried out immediately after the surface treatment.

Adhesion of the coating to the stent wire mesh upon expansion

Once a stent is implanted and expanded, the strained coating has to hold its integrity. As shown earlier in Figure 3 at the final equilibrium point **c**, the coating will be under tension by the struts of the stent framework. The forces have to be in balance so that there is no delamination of the coating from the metal. At present, stents are electropolished as their final finish, which produces a very smooth, corrosion-resistant surface, but if the stents are to be totally encapsulated, then this smooth surface may no longer be needed. In order to test the performance of a simulated coated stent, a model was made for testing in the Instron. A stainless steel wire of 500 μm diameter, was threaded on a jig to form an expandable pattern, as shown in Figure 6. The wire was placed on a pre-prepared thin polyurethane film (~50 μm), and re-coated with polyurethane. High magnification optical images were taken of the wire coating integrity before elongation (Figure 7), where it can be seen that the coating was uniform even around the curves of the wire. The total film thickness of the coating between the wire struts was measured at approximately 125 μm. An optical microscope with a video

camera was set up outside the environmental chamber so that the induced strain was recorded during the tensile test

RESULTS AND DISCUSSION

Stress/strain behavior of polyurethane film

Stress/strain experiments performed on polyurethane films of different thicknesses are shown in Figure 8. In these experiments, the films were loaded to 255 % strain, and then unloaded to zero load. In this plot the unloading strain is not shown for clarity.

The stress was plotted as the force per mm width of the film to correspond with the hoop stress for a coated stent. The stress required to strain each film to 225 % was plotted as a function of film thickness, and is shown in Figure 9. Extrapolation of the plot showed that for a maximum stress (e.g. for a 4 mm balloon-expandable stent expanding to 9 mm in a 7 mm vessel) of approximately 0.11 N/mm the film thickness was ~ 25 - 30 μm. As previously shown by Mazumder *et al*,[18] a 30 μm polyurethane film showed a significant reduction in the corrosion susceptibility of NiTi as used in self-expanding stents.

Another observation from the stress/strain curves was that a residual strain of up to 25 % remained in the films after unloading. This may be attributed to the disruption of the hard segments in the polymer. The chemistry of the hard and soft segments and the degree of phase separation can significantly affect the stress/strain behavior. Hard segment crystallization has been found to increase this hysteresis of the stress/strain curves.[15] Work by Amitay-Sadovsky *et al* [30] showed that the elastic properties of a polyurethane surface is different from that of the bulk for small strains (10 – 20 %), but at higher strains (>100 %) the surface elastic modulus increased along with a decrease in the surface roughness. It was

suggested that randomly oriented hard segments migrate to the surface upon stretching leading to an increase in the hard-to-soft segment concentration and causes a decrease in the surface roughness[30] Phase imaging using Atomic Force Microscopy (AFM) of two components in a similar polyurethane film was shown by De *et al*[19] and clearly showed the distribution of the two segments due to differences in stiffness.

Effect of strain on the surface chemistry and wettability of the polyurethane coating

XPS analysis

XPS data of the carbon peak of polyurethane before and after plasma treatment are shown in Figure 10, and the peak summary is presented in Table 1. Peaks were identified at 284.6, 285.5, 286.5, 288.2, 290.0, and 290.5 eV, corresponding to C-C/C-H, C-N, C-O, C=O, O-C=O, and π-π^* bonding.[31-33] From the data it was observed that there were only minor changes after plasma treatment. There was a decrease in the C-C/C-H bonding and an increase in the C=O bonding indicating an increase in the oxidation of the surface. The synthesis of the ChronoFlex AR is carried out by the addition of MDI to polycarbonate diol, with the addition of a mixture of chain extenders and a molecular weight regulator, of which the composition of the latter two are unknown. Therefore at the present, it is difficult to get an accurate interpretation of the relevance of the plasma induced surface changes from the XPS data. However, identification of the surface functional groups in correlation with surface tension data can enable the amount of hydrophilicity to be determined.

Surface wettability

The Zisman plot of untreated polyurethane and PTFE is shown in Figure 11. The critical surface tension (γ_{crit}) of PTFE was measured at 20.5 dynes/cm, which is in good agreement

with reported values of 18.5 – 22 dynes/cm,[30] and that of the untreated polyurethane was measured at 27 dynes/cm which is within the zone of biocompatibility. The Zisman plot of untreated polyurethane as received and strained to 100 % and 225 % elongation is shown in Figure 12, where the critical surface tension was observed to only increase slightly even for 225 % elongation to ~ 29 dynes/cm, and still within the zone of biocompatibility. It is interesting to observe that the data for the 100 % elongation showed higher values for cos θ, i.e. lower contact angles and hence more hydrophilicity, than for the 225 % elongation film. This is at present unexplained and warrants further investigation. The Zisman plot for untreated and plasma treated films as received and strained to 225 % elongation is shown in Figure 13. Again it was observed that both the plasma treatment and straining the films caused the hydrophilicity to increase, but the critical surface tension was still < 30 dynes/cm, within the zone of biocompatibility.

Adhesion of the coating to the stent upon expansion

Images of part of the wire taken at various points in the test up to 50% strain and on unloading are shown in Figure 14. Stretching of the polyurethane film from the wire was first observed at 13.3 % strain. It appears to be pronounced around a bend in the wire. At 50 % strain, slight separation from the wire is also observed on a straight part of the wire that was not seen in earlier images. Upon unloading, a marked delamination region was observed at 20 % strain; however, this is not so pronounced upon complete unloading (0 %), and the coating appears similar to before the test. As an encased stent is expected to have an improved wire-to-film adhesion, then a plasma or chemically treated stent will be used.

CONCLUSIONS

A method of encasing cardiovascular stents with a radially expandable polyurethane film is developed for its potential application to minimize restenosis. Stress/strain tests show a film < 30 μm thickness is sufficient to prevent re-collapse of a balloon or self-expanding stent. Plasma modification and straining polyurethane films to 225 % does not affect critical surface tension, within the zone of biocompatibility, but showed a slight increase in hydrophilicity which may enhance endothelial cell growth. XPS analysis showed a reduction in C-C/C-H bonding and increase in C=O bonding showing oxidation of the surface. Adhesion tests on smooth stainless steel wire showed some delamination at only 50 % strain.

ACKNOWLEDGMENTS

This work was supported by a grant from the State of Arkansas. The authors gratefully acknowledge Dr. Charles Buhler of ASRC/Kennedy Space Center for the XPS analysis.

REFERENCES

1. American Heart Association, Stent Procedure. http://www.americanheart.org/presenter.jhtml?identifier=4721
2. Grewe P, Denecke T, Machroui A. Acute and chronic tissue response to coronary stent implantation. J Am Coll Cardiol 2000;5:157-163.
3. Dee KC, Puleo DA, Bizios R. An Introduction to Tissue-Biomaterials Interactions. New York: John Wiley & Sons; 2002.
4. FDA News. FDA approves drug-eluting stents for clogged heart arteries. April 2003. http://www.fda.gov/bbs/topics/NEWS/2003/NEW00896.html

5. Herrmann R, Schmidmaier, Märkl GB, Resch A, Hähnel I, Stemberger A, Alt E. Antithrombic coatings of stents using a biodegradable drug delivery technology. Thromb. Haemost. 1999;82:51-57.
6. Szycher M, Armini A, Bajgar C, Lucas A. Drug-eluting stents to prevent coronary restenosis. 2002. http://www.implantsciences.com/pdf/IMXpaperv2-rev2.pdf
7. Kleshinski SJ, Harry JD. Medical stenting: A synthesis of design principles. Nitinol Medical Technologies, Inc., Boston, MA; 1997. p 561-565.
8. Trigwell S, Hayden RD, Nelson KF, Selvaduray G. Effects of surface treatment on the surface chemistry of NiTi alloy for biomedical applications. Surf and Interface Anal 1998;26:483-480.
9. Cisse O, Savadogo O, Wu M, Yahia L'H. Effect of surface treatment of NiTi alloy on its corrosion behavior in Hank's solution. J Biomedical Matls Research 2002;61(3):339-345.
10. Armitage DA, Parker TL, Grant DM. Biocompatibility and hemocompatibility of surface-modified NiTi alloys. J. Biomedical Matls. Research 2003;66A:129-137.
11. Castleman LS, Motzkin SM. In: Williams DF, editor. Biocompatibility of Clinical Implant materials. Vol. 1. Boca Raton: CRC Press; 1981.
12. Miao W, Mi X, Zhu M, Guo J, Kou Y. Effect of surface preparation on mechanical properties of a NiTi alloy. Materials Science Forum 2002;394-395:173-176.
13. Shabalovskaya S, Ryhanen J, Yahia L'H. Bioperformance of nitinol: Surface tendencies. Materials Science Forum 2002;394-395:131-138.
14. Sigwart U, Prasad S, Radke P, Nadra I, Stent coatings. J Invasive Cardiol 2001;13(2):141-142.

15. Lamba NMK, Woodhouse KA, Cooper SL. Polyurethanes in Biomedical applications. Boca Raton: CRC Press; 1998.

16. Mazumder MM, Mehta JL, Mazumder MK, Ali N, Trigwell S, Sharma R, De S. Encased stent for rapid endothelialization for preventing restenosis. Patent Pending. 2004

17. Fact sheet: ChronoFlex® AR: Biodurable medical grade polyurethane, CardioTech Intl. 2004. http://www.cardiotech-inc.com/products/chronoflexar.asp

18. Mazumder MM, De S, Trigwell S, Ali N, Mazumder MK, Mehta JL. Corrosion resistance of polyurethane-coated nitinol cardiovascular stents. J Biomater Sci Polymer Edn 2003;14:1351-1362.

19. De S, Sharma R, Trigwell S, Laska B, Ali N, Mazumder MK, Mehta JL. Endothelial cell growth on plasma-treated polyurethane coated stents for long-term biocompatibility. J Biomater Sci Polymer Edn 2004 Accepted for publication

20. Barrett CR, Nix WD, Tetelman AS. The principles of engineering materials. Englewood Cliffs: Prentice-Hall; 1973

21. Duerig TW, Tolomeo DE, Wholey M. An overview of superelastic stent design. Min Invas Ther & Allied Technol 2000;9(3/4):235-246.

22. Duerig TW, Wholey M. A comparison of balloon and self-expanding stents. Min Invas Ther & Allied Technol 2002;11(4):173-178.

23. Prutton M. Introduction to surface physics. Oxford: Clarendon Press; 1994.

24. Dettre RH, Johnson RE. In: Gould RF, editor. Contact Angle, Wettability, and Adhesion. Washington DC: ACS; 1964

25. Zisman WA. Relation of the equilibrium contact angle to liquid and solid constitution. In: Gould RF, editor. Contact Angle, Wettability and Adhesion, Washington DC: ACS; 1964

26. Baier RE. The role of surface energy in thrombogenesis. Bull NY Acad Med 1972;48:257-272.

27. Adamson AW. Physical Chemistry of Surfaces. New York: John Wiley & Sons; 1982.

28. Fox HW, Zisman WA. The spreading of liquids on low energy surfaces. I. PTFE. J Colloidal Science 1950;514-531.

29. Surface tension values of some common test liquids for surface energy analysis. 2003. http://surface-tension.de/index.html

30. Amitay-Sadovsky, Ward EB, Somorjai GA, Komvopoulos K. Nanomechanical properties and morphology of thick polyurethane films under contact pressure and stretching. J Appl Physics 2002;91(1):375-381.

31. Beamer G, Briggs D. High Resolution XPS of Organic Polymers, The Scienta ESCA 300 database. England: John Wiley & Sons; 1992.

32. Briggs D, Seah MP. Practical Surface Analysis by Auger and X-Ray Photoelectron Spectroscopy. England: John Wiley & Sons; 1983.

33. Li D, Zhao J. Surface biomedical effects of plasma on polyurethane. In: Mittal KL, editor. Polymer Surface Modification: Relevance to Adhesion. Utretch: VSP; 1995. p 137-149.

Figure 1: (a) uncoated versus coated, (b) 3 mm, 5 mm, and (c) 15 mm encased stents.

Figure 2: Circumferential (hoop) stress in a thin walled tube due to internal pressure P.

Figure 3: Cross-section of encased stent showing expansion from **a** to **b** and then recoiling back to final equilibrium at **c** after deflation of the balloon.

Figure 4: (a) Schematic of plasma modification apparatus. (b) Polyurethane film ready for modification.

Figure 5: (a) Schematic side view of carrier for stretched films. (b) Polyurethane film stretched 225 % showing 10 glycerol drops for contact angle measurements.

Figure 6: Schematic of 500 μm stainless steel wire encased in polyurethane film.

Figure 7: Optical images of polyurethane coated stainless steel wire. (a) – (d) topside. (e) – (f) underside.

Figure 8: Stress/strain curves for polyurethane films as a function of film thickness. The stress is plotted as the load per mm of the film width.

Figure 9: Plot of force required to strain a polyurethane film to 225 % as a function of film thickness. The force is plotted as the load per mm of film width.

Figure 10: XPS spectra of the carbon 1s peak before and after plasma modification showing the component peaks.

Figure 11: Zisman plot of PTFE and untreated polyurethane.

Figure 12: Zisman plot of untreated polyurethane as-received and strained to 100 and 225 % elongation.

Figure 13: Zisman plot of untreated and He+ plasma treated polyurethane as-received and after straining to 225 % elongation.

Figure 14: Optical images of a polyurethane coated wire while straining to 50 % elongation at 37 °C.

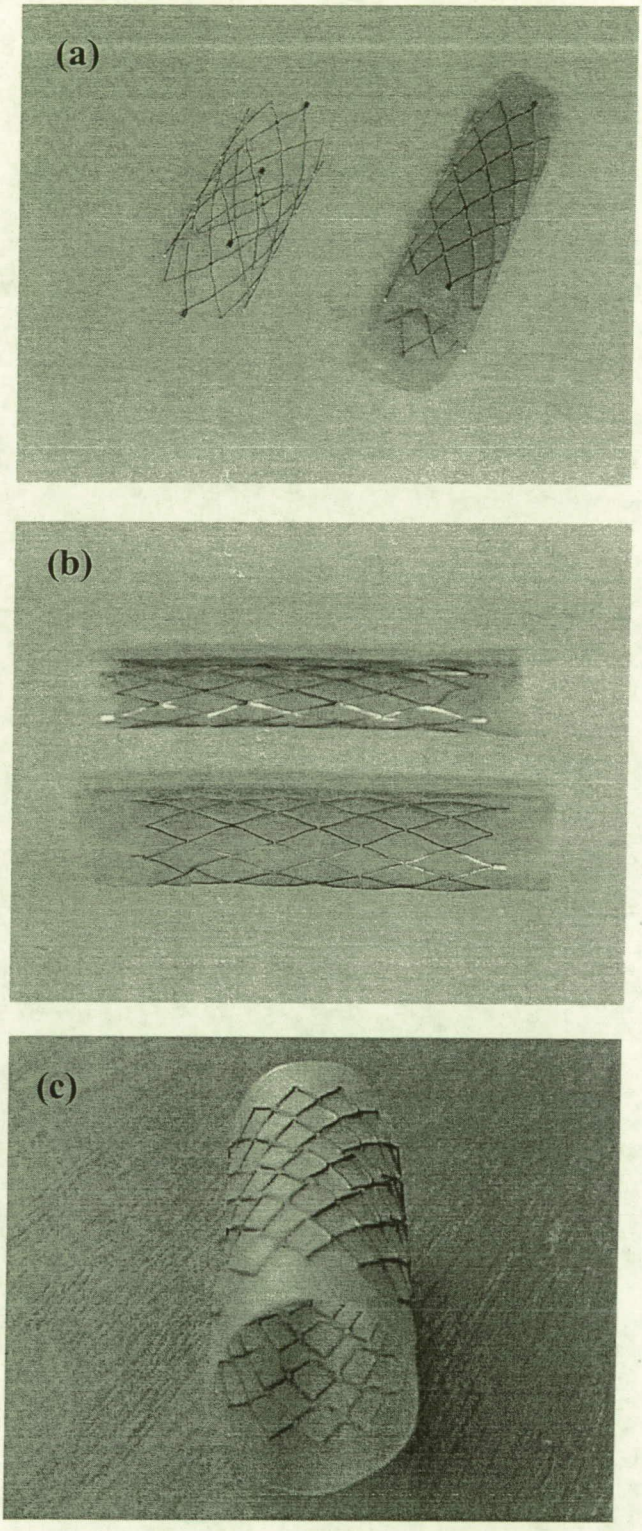

Fig.1

Multiple Pages Missing from Available Version

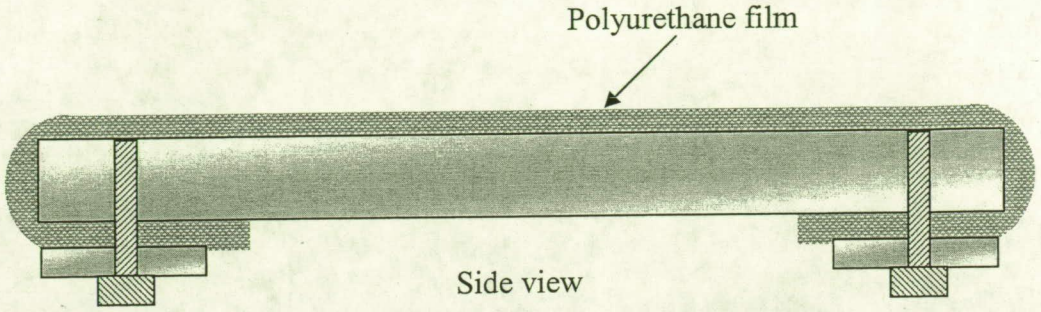

(a)

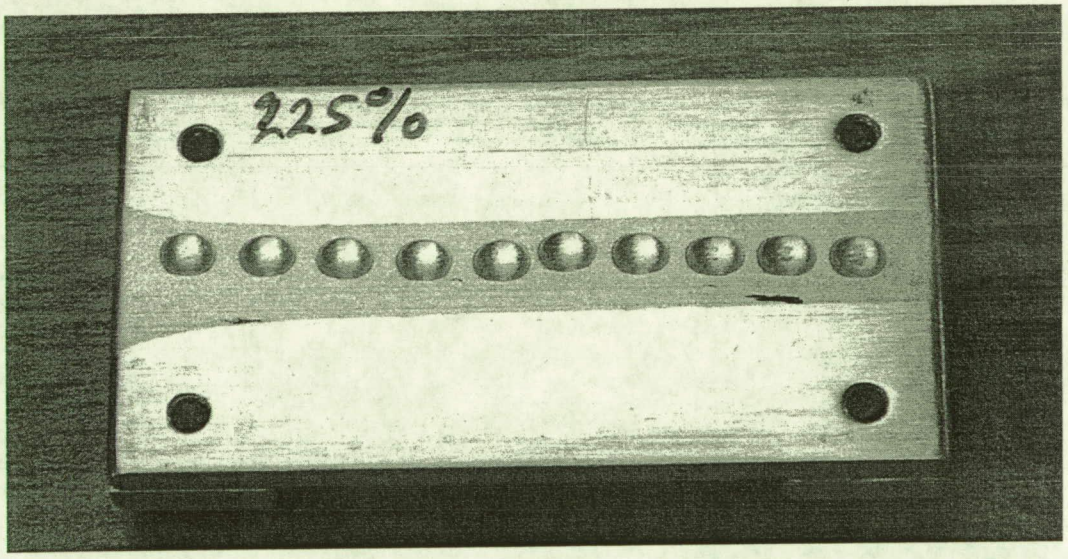

(b)

Fig.5

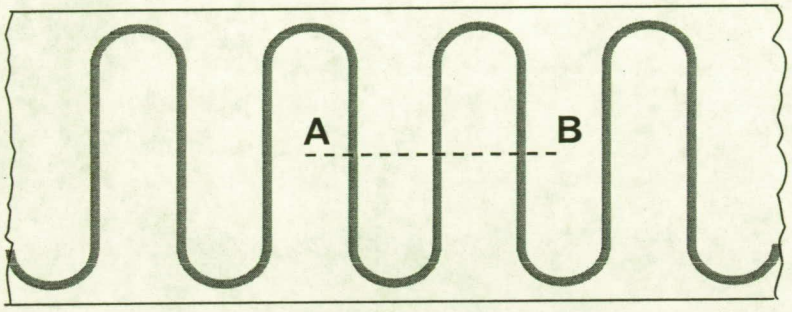

Topside

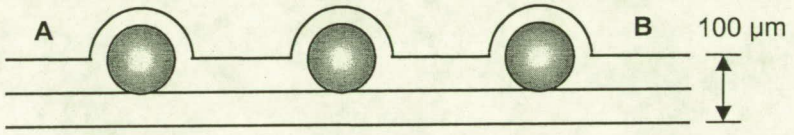

Side view

Fig.6

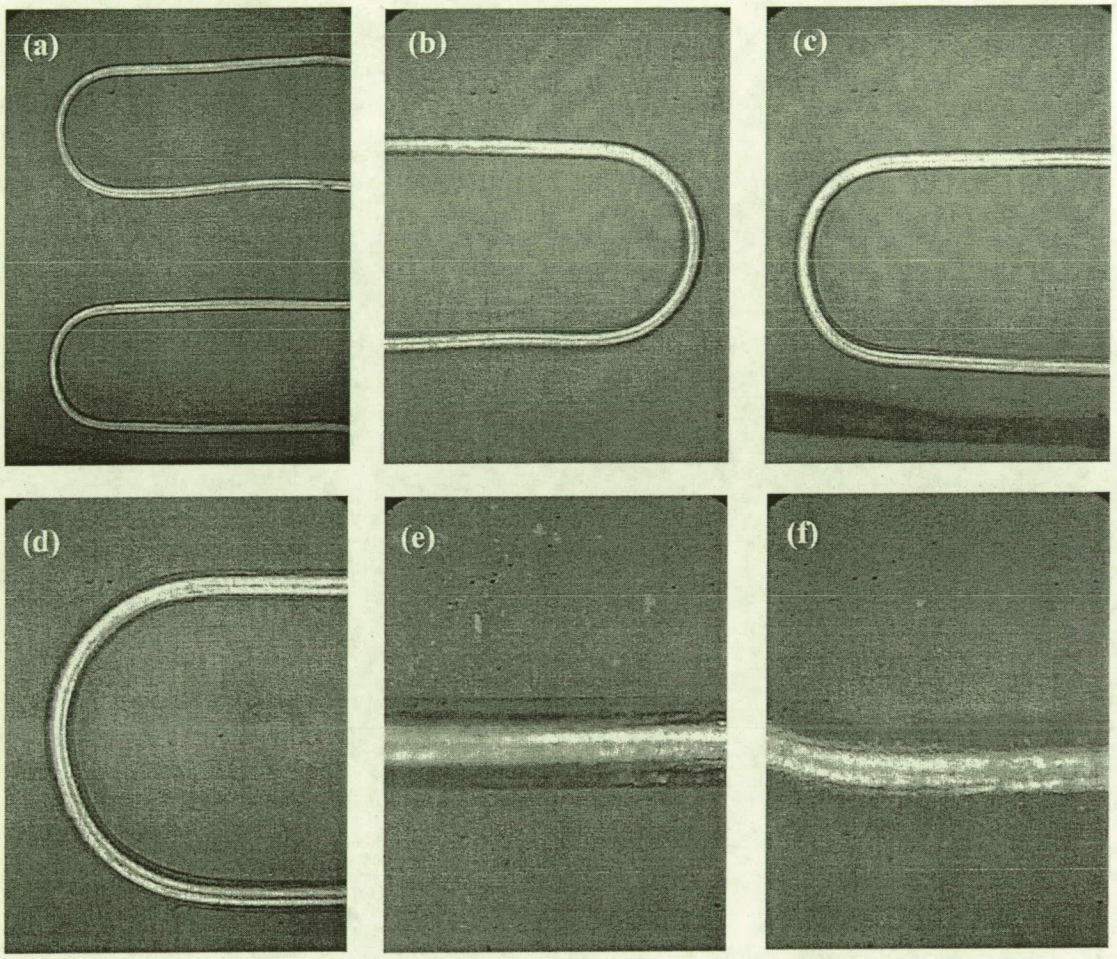

Fig.7

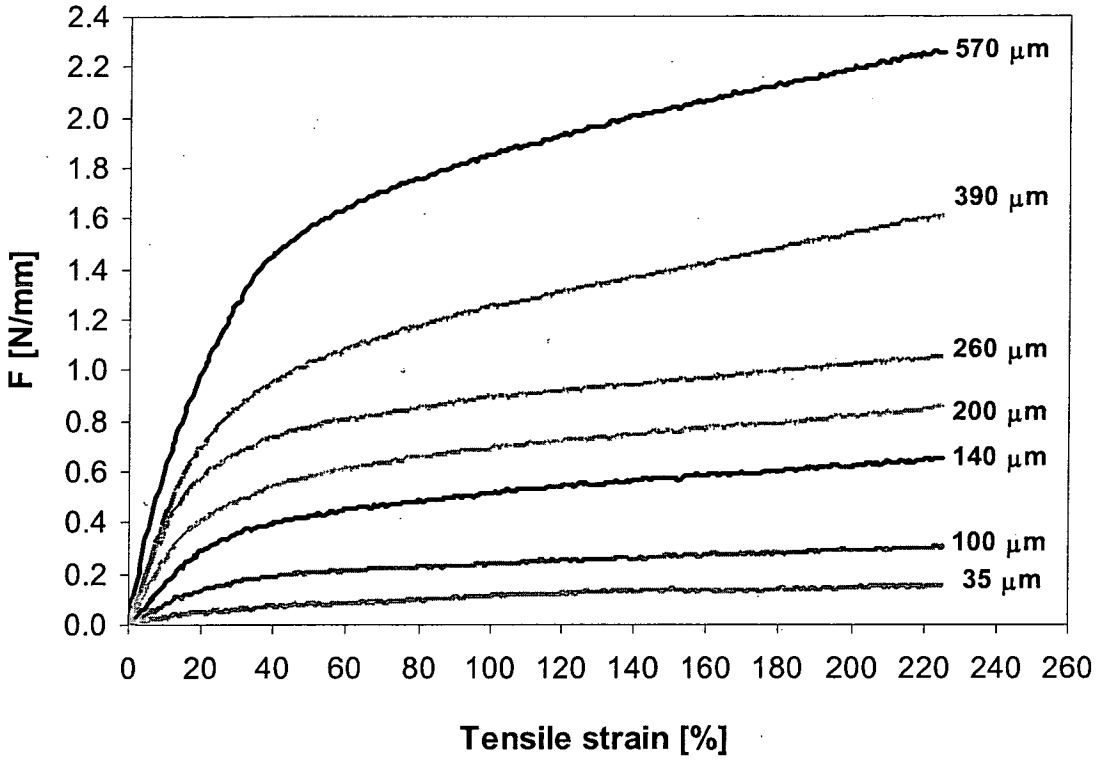
F [N/mm]
2.4
2.2
2.0
1.8
1.6
1.4
1.2
1.0
0.8
0.6
0.4
0.2
0.0
0
20
40
60
80
100
120
140
160
180
200
220
240
260
Tensile strain [%]
570 µm
390 µm
260 µm
200 µm
140 µm
100 µm
35 µm

Fig.8

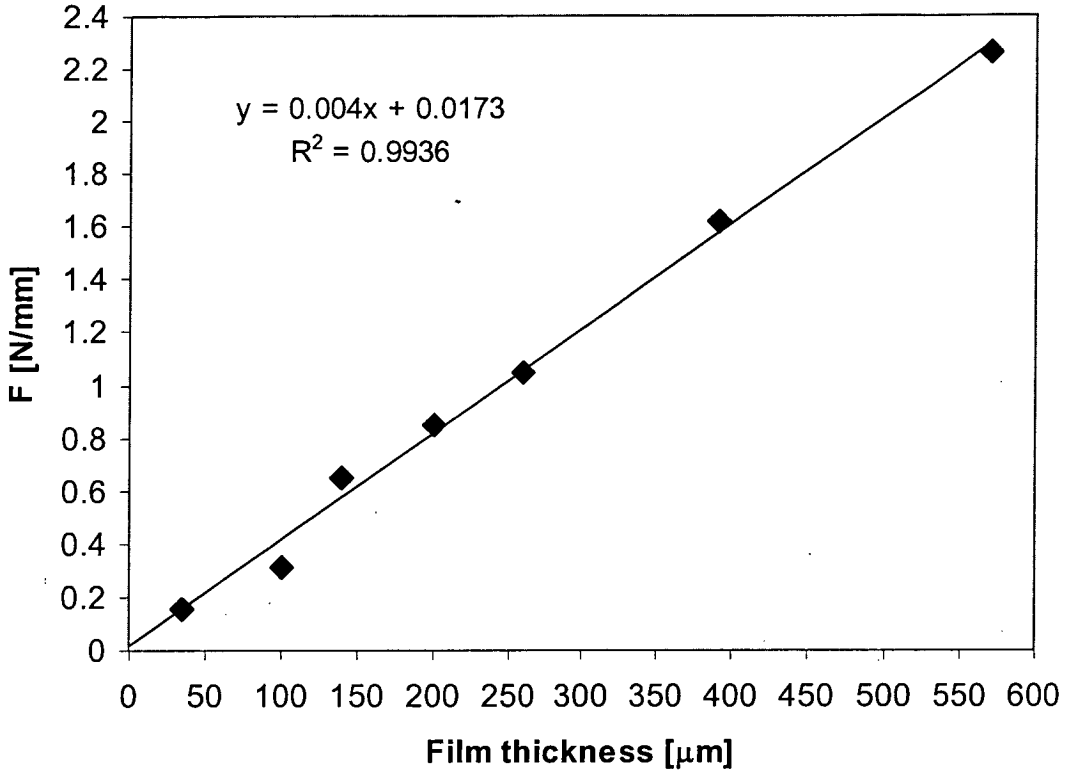
y = 0.004x + 0.0173
R2 = 0.9936
F [N/mm]
Film thickness [μm]
0
0.2
0.4
0.6
0.8
1
1.2
1.4
1.6
1.8
2
2.2
2.4
0
50
100
150
200
250
300
350
400
450
500
550
600

Fig.9

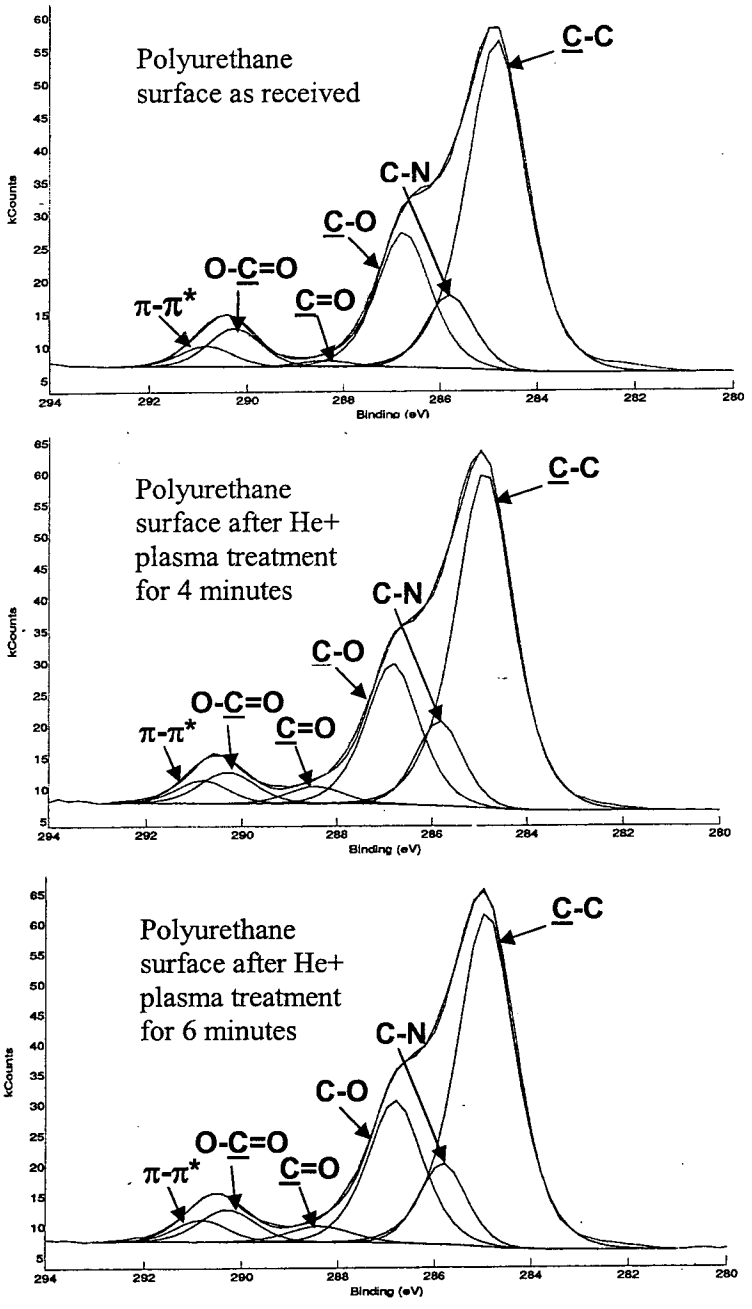
Polyurethane
surface as received
C-C
C-N
C-O
O-C=O
C=O
π-π*
kCounts
Binding (eV)
Polyurethane
surface after He+
plasma treatment
for 4 minutes
C-C
C-N
C-O
O-C=O
C=O
π-π*
kCounts
Binding (eV)
Polyurethane
surface after He+
plasma treatment
for 6 minutes
C-C
C-N
C-O
O-C=O
C=O
π-π*
kCounts
Binding (eV)

Fig.10

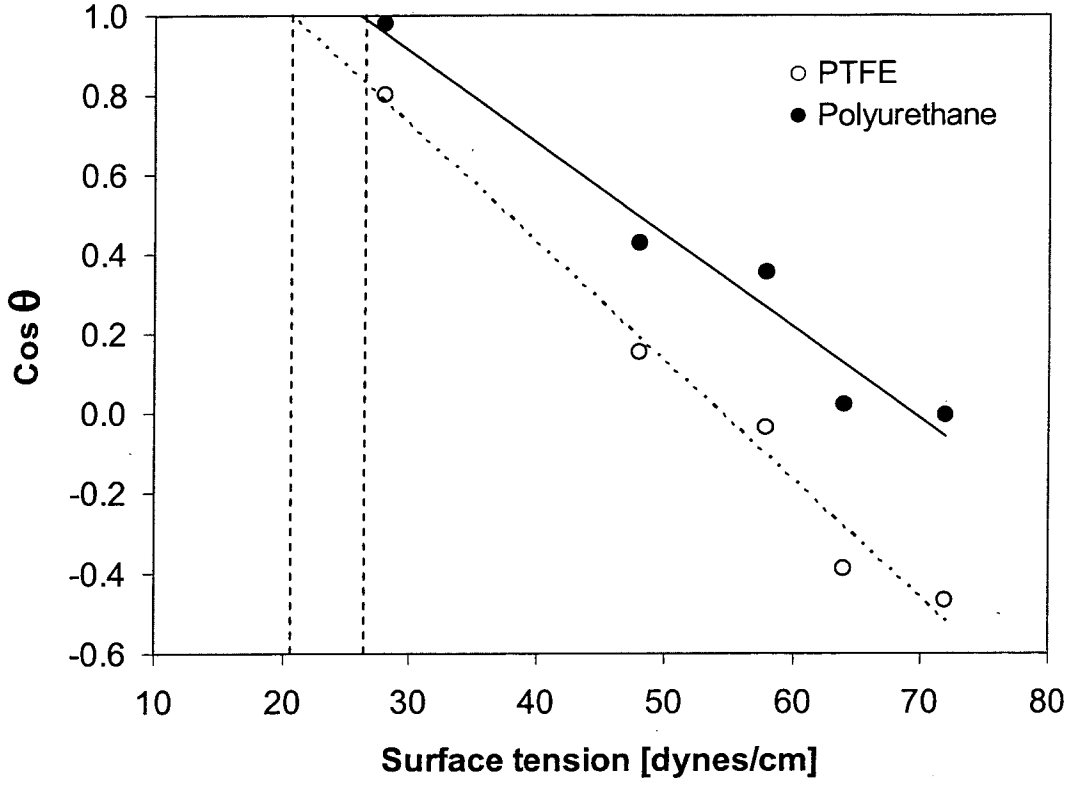
1.0
0.8
0.6
0.4
0.2
0.0
-0.2
-0.4
-0.6
Cos θ
10
20
30
40
50
60
70
80
Surface tension [dynes/cm]
PTFE
Polyurethane

Fig.11

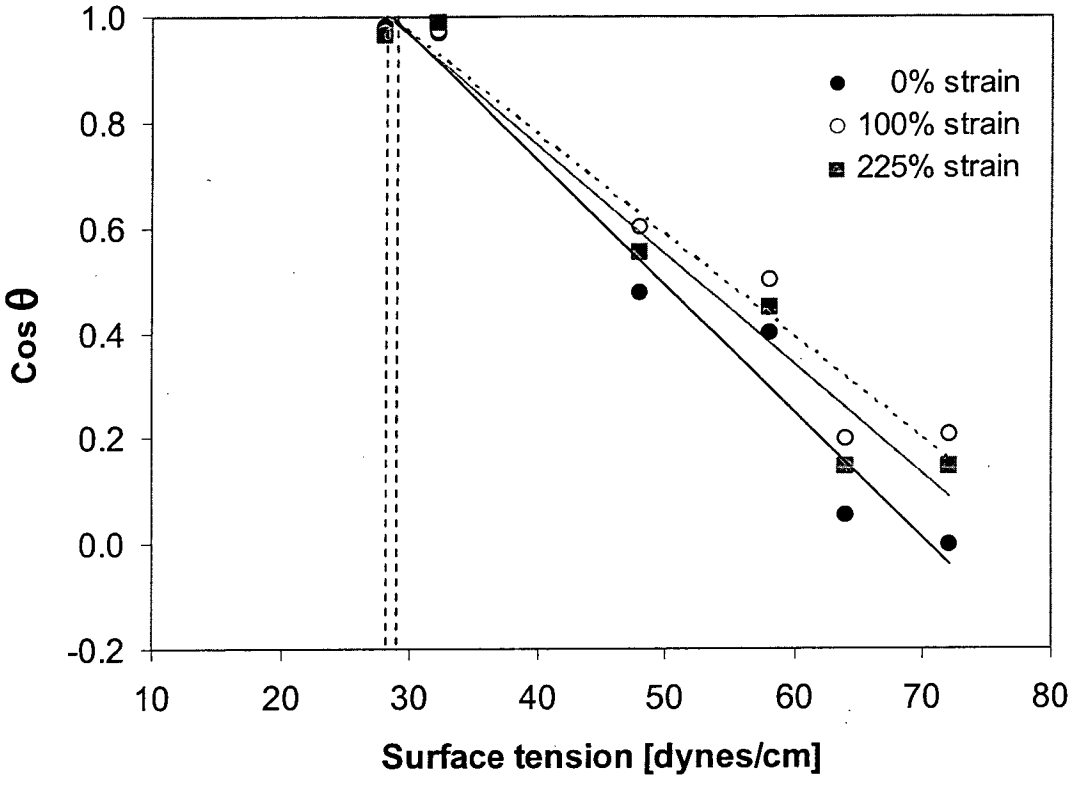
1.0
0.8
0.6
0.4
0.2
0.0
-0.2
Cos θ
10
20
30
40
50
60
70
80
Surface tension [dynes/cm]
0% strain
100% strain
225% strain

Fig.12

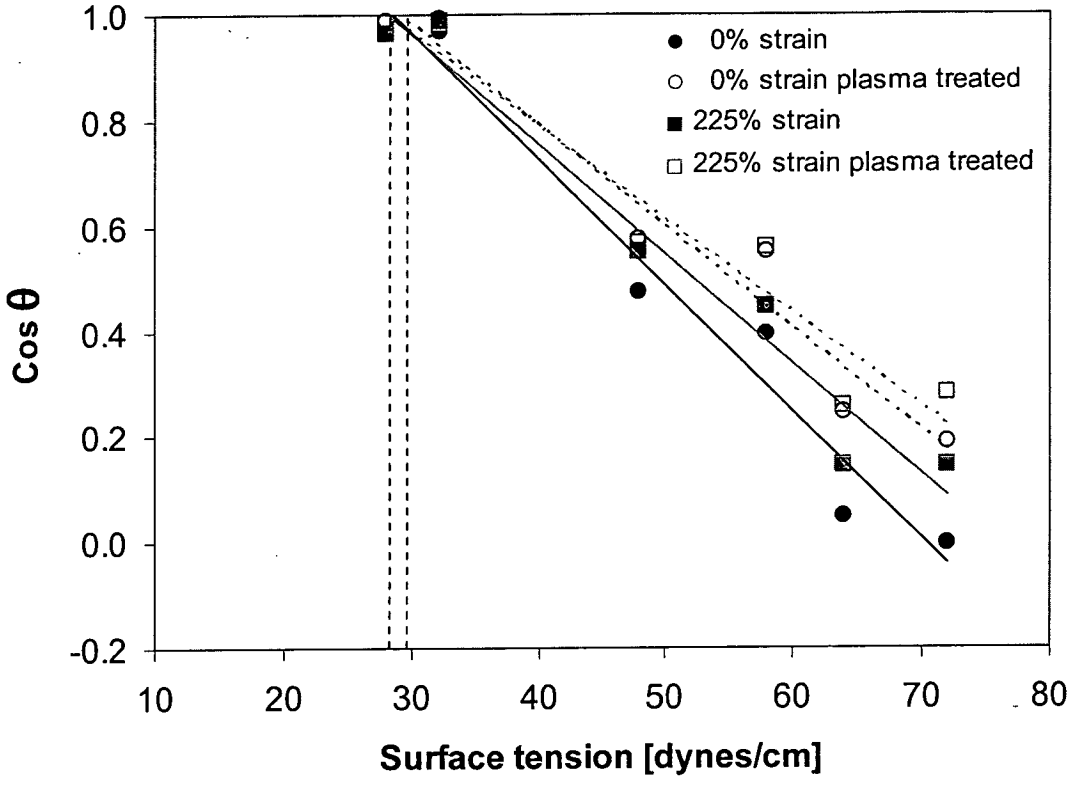
1.0
0.8
0.6
0.4
0.2
0.0
-0.2
Cos θ
10
20
30
40
50
60
70
80
Surface tension [dynes/cm]
0% strain
0% strain plasma treated
225% strain
225% strain plasma treated

Fig.13

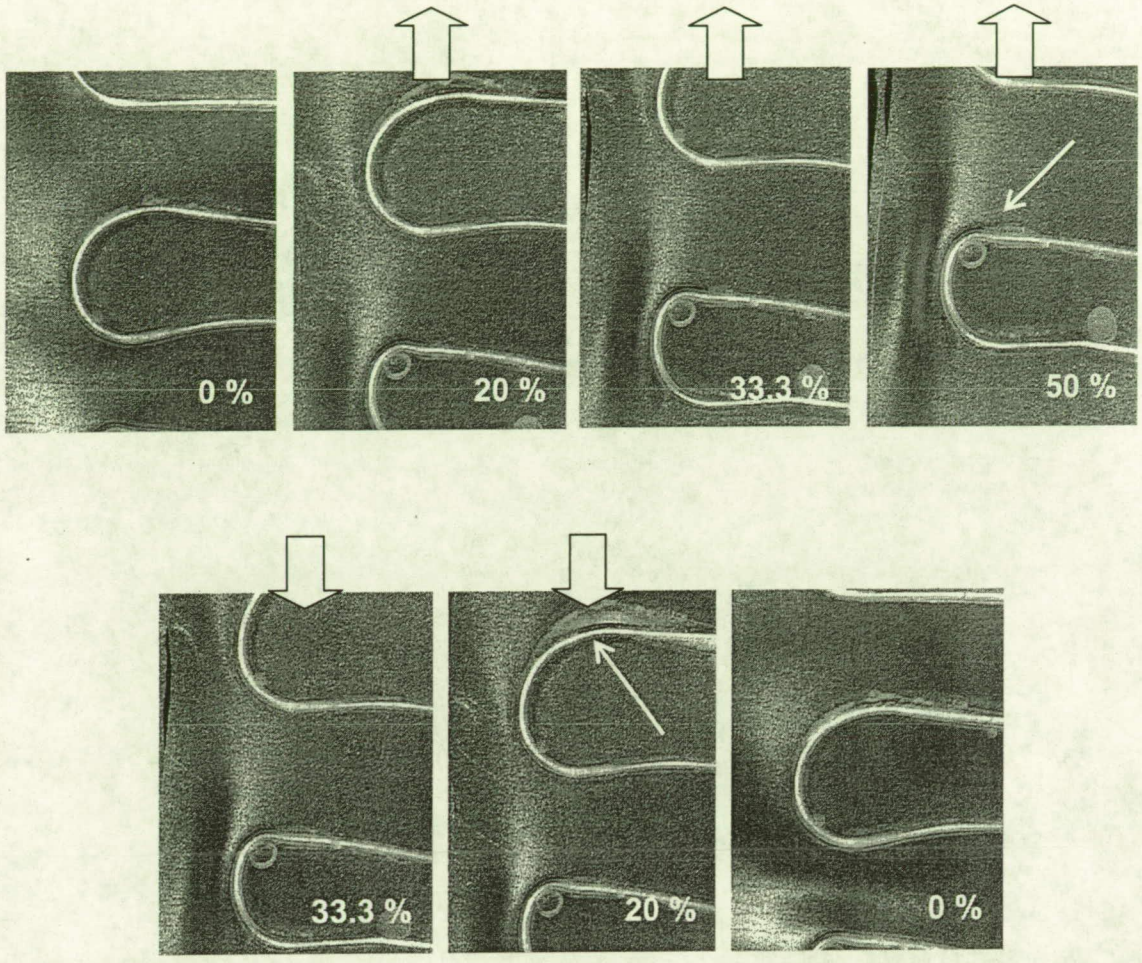

Fig.14

Table 1: Plasma modified surface carbon curve deconvolution summary

	C-C	C-N	C-O	C=O	O-C=O	$\pi - \pi^*$
As received	58.7	10.0	21.7	0.88	5.7	3.0
He+ 4mins.	57.0	10.8	21.7	2.6	4.8	3.2
He+ 6 mins	56.5	10.7	22.0	2.7	4.9	3.1